Effect of Nano-Particle Coating on Marine Propellers

Lalith Sai Madhav Rayala, Surya Sudarsan Naveen Ravula, Amartya Singampali

GVP College of Engineering (A), Visakhapatnam, India.

Abstract:

A *propeller* is a rotating structure used for propulsion using the power generated and transmitted by the main engine. The propellers are subjected to various severities such as corrosion, cavitation and deposition of unwanted waste materials on their surface. It becomes an onerous task to reduce the overall damage and increase the propeller's efficiency. A hydrophobic layer comes in handy in such cases. Aluminium Oxide (Al_2O_3) nanoparticles are considered to fortify the case against the most common cause of propeller deterioration, i.e. corrosion. The chosen coating wards off all marine growth and presents a smooth surface that can withstand friction caused due to water flow when the vehicle is in motion. In the current study, an ellipsoidal model is considered to perform CFD analysis to understand the behavior of lift and drag coefficients of an underwater body. As a part of real-time applications, a propeller body model is considered, and CFD analysis is performed over the body for different angles of attack. The study of the nature of surface coatings is also taken as a part of the project. The modelling is done in CATIA V5 R20 modelling software, and complete CFD analysis is performed using Fluent 15.0.

Keywords: *Nano particle, Propeller, Aluminium Oxide, Computational Fluid Dynamics, Nano coating*

1. Introduction:

Ships, submarines and other underwater equipment like torpedoes and submersibles use propellers for propulsion [10]. A propeller is complex 3D model geometry that transfers power by converting rotational motion into thrust; thus, it is designed to withstand static and dynamic loads [6, 7]. A pressure difference is produced between the forward and rear surfaces of the airfoil-shaped blade, and a fluid (air or water) is accelerated behind the

blade [11]. Propeller dynamics can be modelled by Bernoulli's principle and Newton's third law. A marine propeller is sometimes colloquially known as a screw propeller or screw [3]. Propeller blades come as three-blade, four-blade, and even five-blade propellers. However, three-blade and four-blade propellers are commonly used [5].

Figure 1: Types of propeller blades (a) 3 blade; (b) 4 blade; (c) 5 blade

A propeller is a critical underwater vehicle component that generates the thrust required to propel the vehicle at the desired speeds. Traditionally, underwater vehicles have been fitted with contra-rotating propellers and ducted propellers. At low speeds, these propellers usually function, but as the demand for speed increases, these have to work at high rotational speeds, which induces high blade tip rotational velocities and low-pressure regions. It affects the cavitation of the blade tips and spreads to the blade's surface as the speed increases further and fails to perform efficiently due to top loss in thrust, blade erosion, and noise. Propeller is emerging as a suitable hydrodynamic propulsor for underwater vehicles having speeds due to high cavitation performance, less radiated noise and nominal imbalance torque. Corrosion will also eventually take hold if the boat operates in saltwater. The salt will cause the blades' metal to appear pitted as the salt eats away at them and slowly destroys the metal alloy. If left unaddressed, the pits in the metal will grow and bore a hole in the blades, implying that the propeller has to be replaced entirely [9]. The present project deals with the design of the propeller and applied loads on the propeller.

Nano-coating is a technique of applying a surface layer to repel dry, water and oil particles. They can be found in liquid and solid forms and provide favorable characteristics [1]. Nano Aluminum Oxide (Al_2O_3), because of its high hardness, high strength, good thermal stability, wear resistance, thermal conductivity, insulation and other properties, has been widely used in coatings.

Multiple studies have notified that additive containing 1-2% alumina and other hard nanoparticles can significantly improve scratch and water resistance. The addition of nano-alumina can significantly enhance the coatings' hardness, scratch, and wear resistance. The coating's wear resistance is 2-4 times higher than that of the traditional coatings. Coatings with nano-alumina have excellent insulation properties, widely used in applications of plastics, batteries and electrical machines. Nano-alumina wear-resistant coatings can be made water-based or solvent-based. Alumina coatings are extensively used in transparent plastics, highly polished metal, wood surfaces and other flat materials to improve wear resistance and life [2].

2. **Methodology:**

Initially the model of the propeller is designed in CATIA software. The final model of the propeller is as shown in the fig

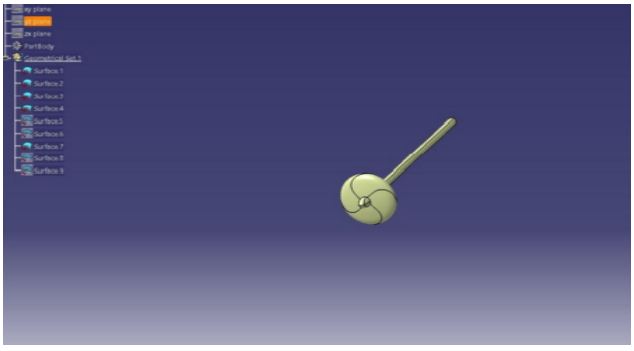

Figure 2: Complete propeller body

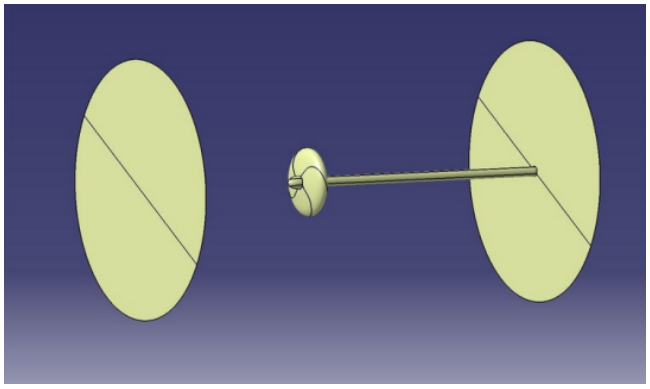

Figure 3: Inlet and outlet of a propeller body

2.1.**Problem-solving steps used in the present analysis:**

The geometry is meshed in ANSYS ICEM CFD as per the given data for each of the models, and a domain is created to encompass the flow inside the domain to the walls of the body. In order to study the domain independence, three cylindrical domains are considered in the trial and error method by taking the distances from the nose and tail end of the model and taking the radius from the axis of the model. Three-dimensional hexahedral grids were generated to discretize the body and the domain.

Three-dimensional segregated implicit solvers are used in the present analysis. The k-□, k-ϵ turbulence models and the continuity and momentum equations were used as governing equations. Boundary conditions used in the present analysis are inlet as velocity inlet, outlet as outflow, far-field, and body as walls. All the three models are computed in the solver Ansys Fluent 15.0.

The solution is iterated until the coefficient of drag(Cd) converges. The solution was stopped when changes in solution variables from one iteration to the next were negligible. The solution is iterated until convergence is observed, obtaining the force and moment results. Since underwater vehicles are similar to ellipsoidal bodies at the ratio of 10:1, we consider an ellipsoidal model.

2.2.**Ellipsoid:**

The model was based on the equation for ellipsoids.

$$(x^2/a^2)+ (y^2/b^2) + (z^2/c^2) = 1$$

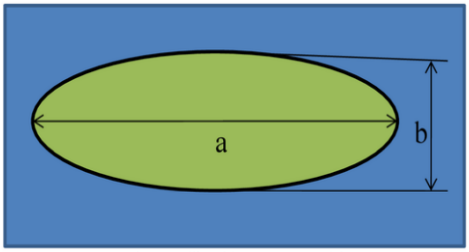

Figure 4: Ellipsoid geometry model

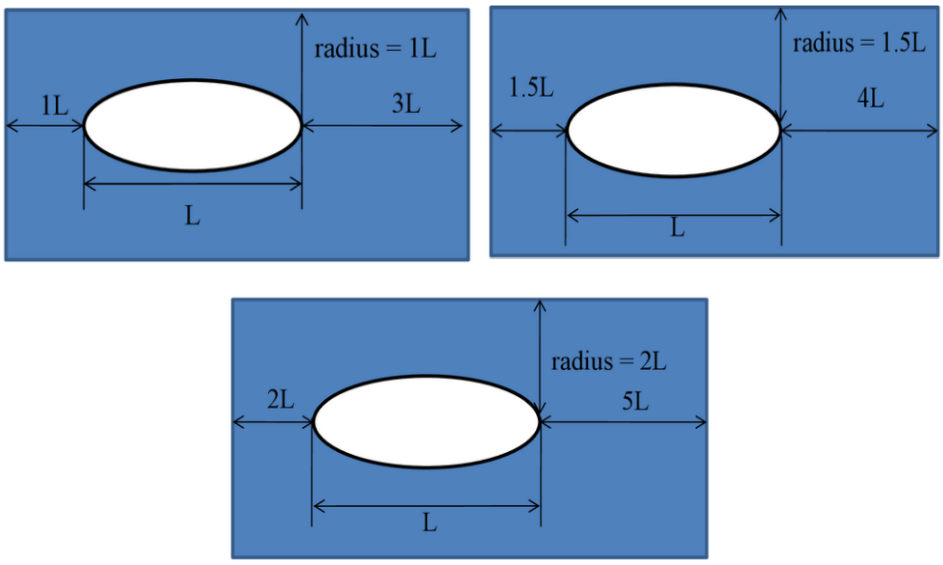

Figure 5: Domains for ellipsoid (a) domain 1; (b) domain 2; (c) domain 3

In the above equation, 'a' is the length of the semi-major axis, 'b' is the length of the semi-minor axis, and b=c for a prolate ellipse and a>b.

a=10m and b=1m

The ellipsoid geometry model is as shown in Figure 4

In order to study domain independence, three cylindrical domains are considered in the trial-and-error method by taking the distances from the nose and tail ends of the model and taking the radius from the axis of the model. The three domains considered are shown in Figure 5

Primarily, the first domain is considered, and a study is carried out, finishing the mesh model, the solver run, the domain independence study, and the grid independence study are carried out.

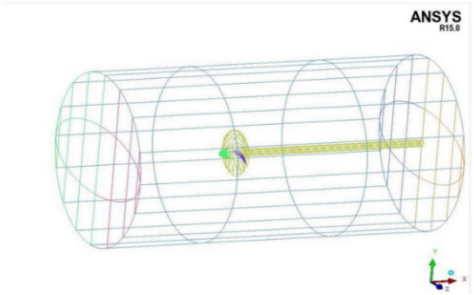

Figure 6: Domain for model simulation

The inlet was considered at a distance of 1L (where L is the length of the ellipsoid model) from the nose end of the ellipsoid model. Similarly, the outlet is considered at a distance of 3L from the tail end of the ellipsoid model. In the radial direction, the domain was considered up to a distance of 1L from the axis of the model.

The mesh was generated, so cell size near the model was small and increased towards the outer boundary.

2.3.**Grid Generation:**

The flow domain must be discretized to convert the partial differential equation into a series of algebraic equations. This process is called grid generation.

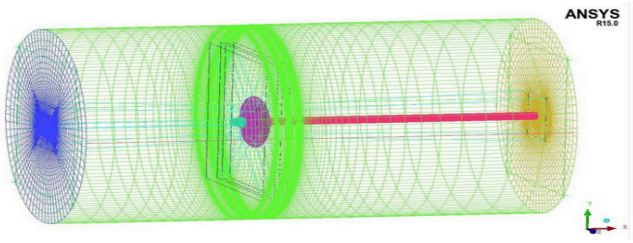

Figure 7: Body grid and its domain

For this model, the ellipsoid is regarded as a solid region, while the region surrounding the model is regarded as the Fluid region. Using block splitting at 'Prescribed Point", generate a hexahedral mesh for both the regions so that the topology of the solid region is to degenerate 'Hexahedral' mesh.

ANSYS ICEM CFD module is started, and the geometry file is imported into the module. The subsequent step is to create a bounding box, i.e., a control volume, to create different parts and assign the different surfaces of the geometry to the appropriate part. Volume

blocks are created, and vertices are associated with points to fit the initialized blocking more closely to geometry.

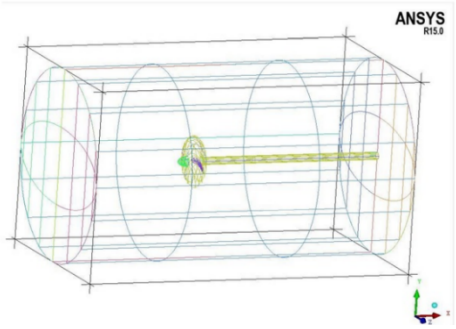

Figure 8: O-Grid blocking

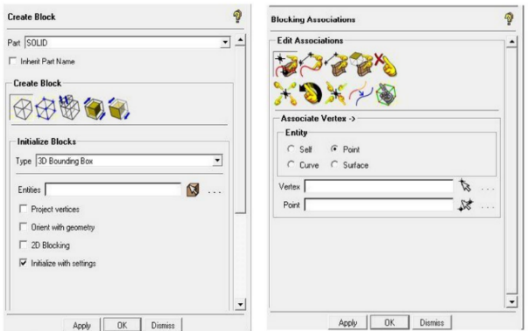

Figure 9: Blocking windows (a) Block generation; (b) Block association

The edges are projected to their respective curves and surfaces. All vertices are snapped and moved to align into respective positions.

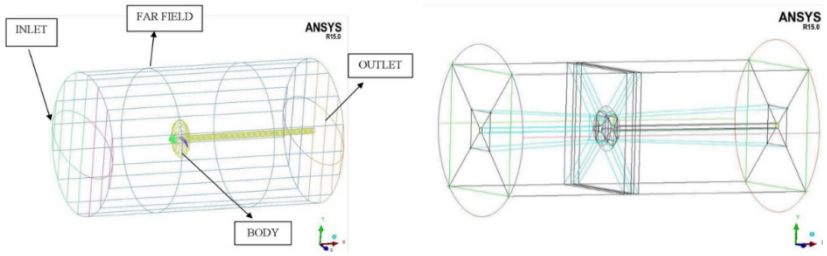

Figure 10: (a)Surface part assignment; (b) Snapping of projected vertices

The next step is to generate mesh to proceed further. The grid is uniformly distributed from the nose end to the tail end of the body. The grid quality is checked and finalized, and the output is saved as a .msh file to the solver. The properties of Nanoparticles are applied to the layer of the propeller, and the flow is initiated from the inlet (velocity-inlet) with the particular velocity of 5 m/s, and the fluid flows out from the outlet (outflow).

The boundary conditions are initiated at different angles of attacks, and the flow analysis is performed.

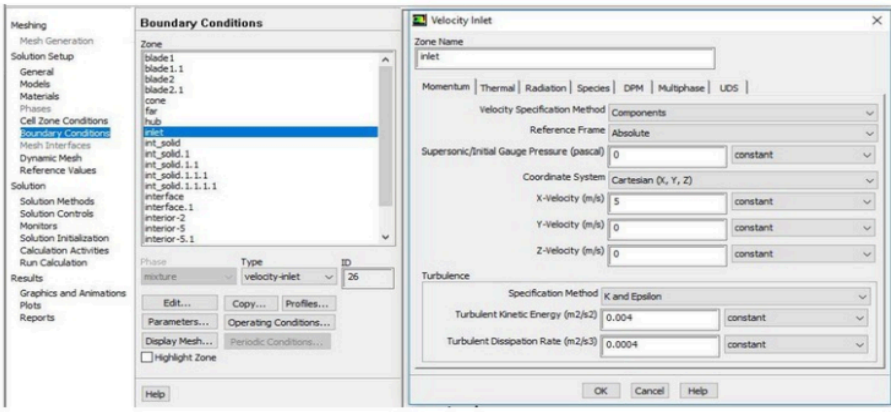

Figure 11: Boundary conditions in ANSYS Fluent

Table 1: Boundary Conditions

ZONE	TYPE
Inlet	Velocity-Inlet
Far	Velocity-Inlet
Body	Wall
Outlet	Outflow
Solid	Fluid

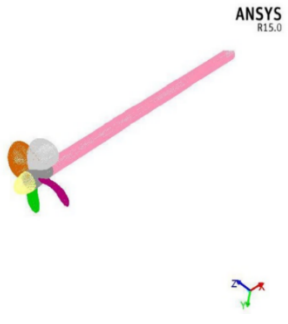

Figure 12: Final Mesh

The properties of Nanoparticles are applied to the layer of the propeller and the flow is initiated from the inlet (velocity inlet) with the particular velocity of 5m/s and the fluid flows out from the outlet (outflow). The boundary conditions are initiated at different angles of attacks and the flow analysis is performed.

Table 2: Nano particle properties

Nano Particle	**Thermal Conductivity (W/mK)**	**Density ($Kg.m^3$)**	**Specific Heat Capacity (J/KgK)**
Al_2O_3	40	4000	765

3. Results and Discussion:

3.1. Pressure Distribution for a propeller blade:

The figure shows the pressure distribution on the surface of the propeller blade for 0° angle of attack, and similarly, 2°,4°,6°and 8° angles are also performed. The nose and tail ends are experiencing high and low pressure, respectively. There is a concentration of high-pressure region near the nose end of the Propeller blade.

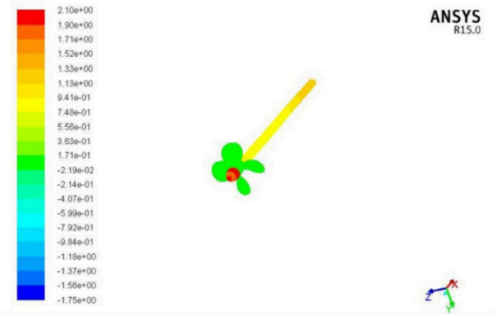

Figure 13: Pressure distribution of propeller blade without coating

3.2. Velocity Vector Distribution:

Velocity vectors enable us to check the fluid flow over the body in the exact direction from the inlet to the outlet given according to the boundary conditions. The figure shows

the velocity vectors over the propeller blade body and the velocity vectors at the nose end of the propeller blade.

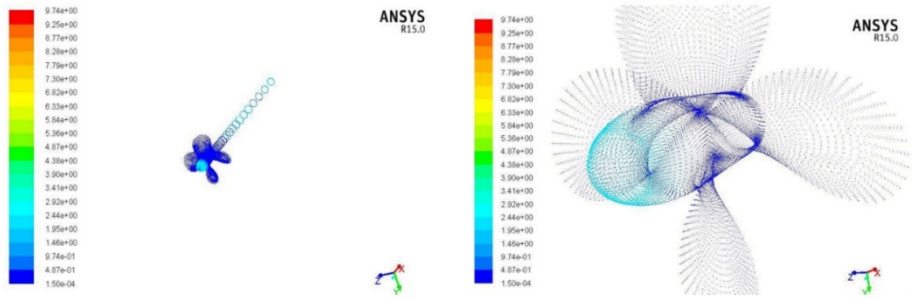

Figure 14: Velocity vectors of propeller blade without coating (a) over the body; (b) nose end

Table 3: Drag and Lift coefficients for different angle of attacks for a propeller blade without coating

Angle of Attack	Coefficient of Drag (C_d)	Coefficient of Lift (C_l)
0˚	0.02682	0.00253
2˚	0.03965	0.00461
4˚	0.06041	0.00661
6˚	0.08299	0.00980
8˚	0.09502	0.02581

3.3.**Results for Propeller with Coating:**

The layer of the propeller is coated with Nano Aluminium Oxide (Al2O3 Nano Particles). The pressure distribution at different angles of attack is analyzed figure15 shows the pressure distribution on the blade's surface for a 0-degree angle of attack. Similarly, 2, 4, 6 and 8 degrees are also performed. The figure16(a) shows the velocity vectors to check the flow of fluid over the body in the exact direction from the inlet to the outlet; figure16(b) shows the velocity vectors at the nose end of the propeller blade.

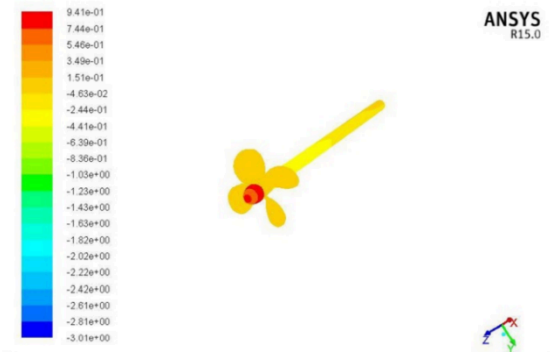

Figure 15: Pressure distribution of propeller blade with coating

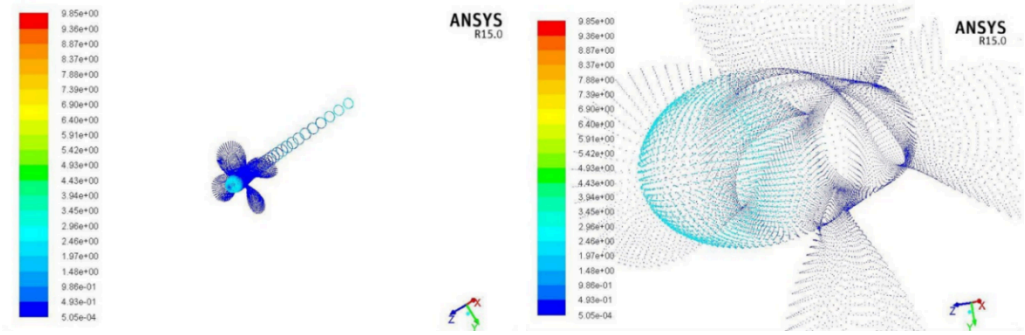

Figure 16: Velocity vectors of propeller blade with coating

(a) over the body; (b) nose end

Table 4: Drag and Lift coefficients for different angle of attacks for a propeller blade with coating

Angle of Attack	Coefficient of Drag (C_d)	Coefficient of Lift (C_l)
0˚	0.02443	0.00216
2˚	0.02657	0.00416
4˚	0.03772	0.00619
6˚	0.04438	0.00897
8˚	0.06091	0.02140

4. Conclusions:

The domain independence and grid independence study are carried out on the ellipsoid model to obtain convergence. After convergence, domain 2 and grid 1 are selected for further analysis. Further, the computational study comprehended the coefficient of drag and the coefficient of lift for the propeller. Furthermore, the results obtained for the propeller with nano-coating have shown promising results compared with the propeller

with no coating. The results show that the coefficient of drag and the coefficient of lift have decreased by 32.32% and 11.37%, respectively, after nano-coating on the propeller blade.

5. **References:**

[1]https://www.twi-global.com/technical-knowledge/faqs/what-is-nano-coating#:~:text=Nano%2Dcoating%2C%20also%20known%20as,provide%20characteristics%20that%20are%20favourable.

[2]http://www.oxidepowders.com/product/nano-aluminum-oxide-for-coating-al2o3/

[3]T. Chittaranjan Kumar Reddy, K. Nagaraja Rao, "Design and Simulation of a Marine Propeller", IJRAET, Volume 5, Issue 1, September 2015.

[4] Gopichand Allaka, B.D.P.P.S.L Anasuya, Ch. Yamini, N.N. Vaidehi, Y. Venkata Ramana, "Modelling and Analysis of Multicopter frame and propeller", Volume 2, Issue 4, Apr 2013. [ansys methodology]

[5] www.marineinsight.com

[6] Praveen Kumar Surisetti, M Lakshmi Sramika, V Srinivas, "Modelling and Analysis of Propeller Blade with CFRP Material by Using Finite Element Analysis".

[7] A. Satya Dinesh, G.V. Naga Mani, "Modelling and analysis of shaft blade for its strength", IJSR, Volume 5, Issue 2, February 2016.

[8]https://www.hsmarineprops.com/blog/2021/3/22/common-problems-with-boat-propellers

[9] M. L. Pavan Kishore, R. K. Behera, Sreenivasulu Bezawada, "Structural analysis of NAB propeller replaced with composite material", International Journal of Modern Engineering Research (IJMER), Volume 3, Issue 1, Jan-Feb 2013.

[10] Shaik Azmatuullah Rahaman, Dr S. Selvarajan, Y.N.V Santosh Kumar, "Design, Development and Analysis of Advanced airboat propeller using Bamboo Composite Fibre Material", IJEDR, Volume 2, Issue 4, 2014.